7-18-2019

Improving Performance of the SMD Solvation Model: Bondi Radii Improve Predicted Aqueous Solvation Free Energies of Ions and pK_a Values of Thiols

Saber Mirzaei
Marquette University

Maxim Vadimovich Ivanov
Marquette University

Qadir K. Timerghazin
Marquette University, qadir.timerghazin@marquette.edu

Journal of Physical Chemistry : A, Vol. 123, No. 44 (July 18, 2019): 9498-9504. DOI.

Improving Performance of the SMD Solvation Model: Bondi Radii Improve Predicted Aqueous Solvation Free Energies of Ions and pK_a Values of Thiols

Saber Mirzaei
Department of Chemistry, Marquette University, Milwaukee, Wisconsin
Maxim V. Ivanov
Department of Chemistry, Marquette University, Milwaukee, Wisconsin
Qadir K. Timerghazin
Department of Chemistry, Marquette University, Milwaukee, Wisconsin

Abstract

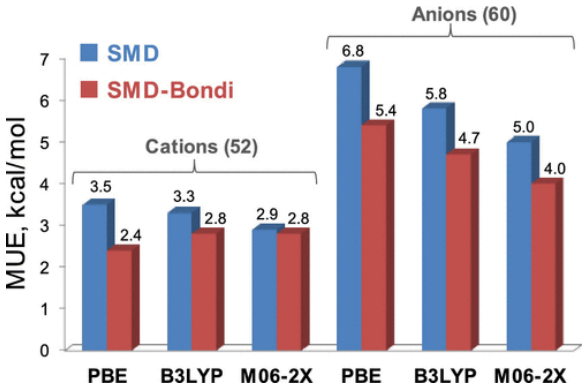

Calculation of the solvation free energy of ionic molecules is the principal source of errors in the quantum chemical evaluation of pK_a values using implicit polarizable continuum solvent models. One of the important parameters affecting the performance of these models is the choice of atomic radii. Here, we assess the performance of the solvation model based on density (SMD) implicit solvation model employing SMD default radii (SMD) and Bondi radii (SMD-B), a set of empirical atomic radii developed based on the crystallographic data. For a set of 112 ions (60 anions and 52 cations), the SMD-B model showed lower mean unsigned error (MUE) for predicted aqueous solvation free energies (4.0 kcal/mol for anions and 2.4 kcal/mol for cations) compared to the standard SMD model (MUE of 5.0 kcal/mol for anions and 2.9 kcal/mol for cations). In particular, usage of Bondi radii improves the aqueous solvation energies of sulfur-containing ions by >5 kcal/mol compared to the SMD default radii. Indeed, for a set of 45 thiols, the SMD-B model was found to dramatically improve the predicted pK_a values, with ∼1 pK_a unit mean deviation from the experimental values, compared to ∼7 pK_a units mean deviation for the SMD model with the default radii. These findings highlight the importance of the choice of atomic radii on the performance of the implicit solvation models.

Introduction

The pK_a value is one of the most important parameters determining the reactivity of (bio)organic molecules, and accurate computational predictions of the pK_a values have been a topic of long-standing interest.(1) Due to the computational costs of including explicit solvent molecules, the electronic structure calculations of the pK_a values mostly rely on the polarizable continuum description of the solvent. In these calculations, inaccurate evaluation of the solvation free energies of neutral molecules and their conjugated ions is one of the main sources of error in the predicted pK_a values.(1−4)

During the past decades, several implicit solvation models (e.g., IEF-PCM,(5) C-PCM,(6) COSMO,(7) etc.) were devised based on the polarizable continuum model (PCM) of Tomasi(8,9) that solves the nonhomogeneous Poisson equation (NPE) to simulate bulk electrostatic effects of the solvent. Alternatively, some other implicit solvation models (e.g., SM8(10) and SM12(11)) are designed in a way to represent the solute as a collection of point charges. These models use the generalized Born approximation(12,13) based on the partial atomic charges.

Accurate simulation of bulk electrostatic interactions is critical for accurate prediction of solvation free energies, particularly in the case of charged solutes. These bulk electrostatic contributions are included into the final solvation free energies with the aid of a cavity that represents a solvated molecule by a dielectric medium. This cavity is defined by a superposition of nuclear-centered spheres with the assigned radius to each atom of the solute. It has been previously shown that nonoptimal atomic radii may significantly deviate the calculated solvation free energies and, in turn, the calculated pK_a values form the experimental data.(14−19)

Regarding the importance of the selected atomic radii, Fang and co-workers attempted to modify the van der Waals radii employed in the integral equation formalism variants of the polarizable continuum model (IEF-PCM) to obtain improved results for neutral molecules.(14,15) Also, in the processes of parametrization of the SM8 solvation model and comparing its performance with other implicit solvation models, Marenich et al. tested four different sets of radii (UA0, UAHF, UAHF*, and Bondi) using the IEF-PCM solvation model to calculate the errors of solvation free energies of 60 anions and 52 cations.(10) Among the four sets of radii tested with IEF-PCM, Bondi radii resulted in the lowest mean unsigned errors (MUE) for both anions (5.5 kcal/mol) and cations (3.7 kcal/mol). Bondi radii have been determined based on the crystallographic data using nonbonded intermolecular distances in the crystal structure of molecules collected at 0 K to represent the highest reliable densities.(20) In spite of the better performance of Bondi radii for the IEF-PCM solvation model, these values were higher than the SM8 mean unsigned error (MUE), 3.7 and 2.7 kcal/mol for anions and cations, respectively.

Another strategy, besides manipulating the atomic radii, to improve the accuracy of the implicit solvation models and the pK_a values, is to explicitly include solvent molecules (most commonly, water) into the calculation along with the implicit solvation model. Such a hybrid model (i.e., implicit + explicit) demonstrates significantly improved results and circumvents the utilization of the thermodynamic cycles (i.e., molecules are optimized both in a solvent and in vacuo);(21) however, it requires more computational resources.(22−28)

Among several implicit solvation models, a solvation model based on density (SMD),(29) which was designed as a universal solvation model (where “universal” denotes its applicability to both ionic and neutral solutes in any solvent), gained a significant popularity for the calculation of condensed phase properties like pK_a values.(30−37) Recently, Schlegel and co-workers showed that utilization of the implicit SMD solvation model with up to three explicit water molecules improves predicted pK_a values of several functional groups relative to implicit-only calculations.(38−41) However, the values obtained without explicit water molecules demonstrated large errors, which suggest poor reliability of the pure implicit SMD solvation model for predicting the pK_a values.

Motivated by the reports on the low MUEs when Bondi radii are employed with the IEF-PCM model(10) and the aforementioned deficiencies of the SMD model without explicit water molecules, here, we explored the performance of the SMD model with Bondi radii. We first investigated the effects of using Bondi radii with the SMD solvation model (SMD-B) on calculations of the aqueous ionic solvation free energies as well as evaluated the application of Bondi radii for predicting the pK_a values of 45 thiols.

We found that using Bondi radii instead of the default SMD radii leads to more accurate values of the calculated aqueous solvation free energies of ions, anions in particular, where the MUE decreases by ∼1 kcal/mol. Importantly, we conclude that it may be beneficial to employ radii that are specifically parameterized for a given charge state of a solute and type of a solvent.

Computational Details

All calculations were performed using Gaussian 09,(42) which uses the integral equation formalism variant of the polarizable continuum model (IEF-PCM)(5) as the default algorithm for the SMD calculations.(29) This model divides the standard free energies of solvation into three components (eq 1)

$$\Delta G^{\circ}_{\mathrm{sol}}\mathrm{v} = \Delta G_{\mathrm{ENP}} - G_{\mathrm{CDS}} + \Delta G^{\circ}_{\mathrm{Conc}} \quad (1)$$

The first component (ΔG_{ENP}) originates from the integration of the nonhomogeneous Poisson equation (NPE) based on the self-consistent reaction field to consider the bulk electrostatic effects. ΔG_{ENP} accounts for the electronic (E), nuclear (N), and polarization (P) effects. The generated cavity around the solute for ENP components (electrostatic effects) results from the superpositions of nuclear-centered spheres based on the

assigned atomic radii to different atoms. Therefore, as listed in Table1, different implicit (continuum) solvation models (e.g., C-PCM,(6) SM12,(11) COSMO,(7) and SMD(29)) use different atomic radii.

Table 1. Various Coulomb radii (Å) Used in Various Solvation Models and the Bondi van der Waals Radii (Å)

atom	C-PCM	SM12	COSMO	SMD	Bondi
H	**1.44**	**1.02**	**1.20**	**1.20**	**1.20**
C	**2.04**	**1.57**	**1.50**	**1.85**	**1.70**
N	**1.92**	**1.61**	**1.50**	**1.89**	**1.55**
O	**1.80**	**1.52**	**1.40**	**1.52**	**1.52**
F	**1.62**	**1.47**	**1.35**	**1.73**	**1.47**
Si	**2.40**	**2.10**	**1.17**	**2.47**	**2.10**
P	**2.28**	**1.80**	**1.80**	**2.12**	**1.80**
S	**2.22**	**2.12**	**1.75**	**2.49**	**1.80**
Cl	**2.17**	**2.02**	**1.70**	**2.38**	**1.75**
Br	**2.34**	**2.60**	**1.80**	**3.06**	**1.85**

The second component is the cavity–dispersion–solvent structure (CDS) term that models the solute–solvent short-range interactions. The G_{CDS} takes into account additional interactions (e.g., dispersion, hydrogen bonding, exchange repulsion, etc.) that are not defined by the electrostatic term.

The last term (ΔG_{conc}°) accounts for the changes upon transferring the solute from the gas phase to the solution. However, here this value is zero due to the same concentration (1 mol/L) of gaseous and solution phases.(43)

In the SMD calculations, the radii scaling factor was set to α = 1.0 for the calculations using Bondi radii (Figure S1 in the Supporting Information (SI)). Vibrational frequency calculations have been performed for all of the fully optimized structures to ensure the absence of imaginary frequencies. In this work, we used a set of six most popular density functionals including pure (Perdew–Burke–Ernzerhof (PBE) and BLYP),(44,45) hybrid GGA (B3LYP, PBE0, and ωB97XD),(45−47) and hybrid meta-GGA (M06-2X)(48) functionals, along with five double- and triple-ζ quality basis sets (6-31G*, 6-31+G*, cc-pVTZ, aug-pcseg-2, def2-TZVPPD).(49−51) To examine the effect of the contribution of the exact (Hartree–Fock, HF) exchange component, M06-HF, M06, and M06-L functionals were tested with the 6-31G* basis set.(48,52,53) A set of 112 ions (60 anions and 52 cations, MNSol data set)(54) with known experimental solvation free energies was used (Tables S3–S6 in the Supporting Information). The pK_a values were calculated using the direct method (which does not require the gas-phase optimization) using eqs 2 and 3

$$\mathrm{p}K_a = \frac{\Delta G^*_{\mathrm{aq}}}{2.303RT} \quad (2)$$

(3)

$$G^*_{\mathrm{aq}} = G^*_{\mathrm{aq}}(\mathrm{A}^-) - G^*_{\mathrm{aq}}(\mathrm{HA}) + G^*_{\mathrm{aq}}(\mathrm{H}+) \quad (3)$$

where G_{aq}^* is the Gibbs energy difference of a deprotonation reaction (HA → A^- + H^+) in the solution, $G_{aq}^*(A^-)$ and G_{aq}^*(HA) are calculated free energies of deprotonated and protonated acids; the aqueous phase free energy of proton $G_{aq}^*(H^+)$ was set to −270.29 kcal/mol, which is the summation of $\Delta G_{solv}(H^+)$ = −265.9 kcal/mol, $G^\circ(H^+)$ = −6.28 kcal/mol, and $\Delta G^{\circ\rightarrow *}(H^+)$ = +1.89 kcal/mol.(55−58)

Results and Discussion

Performance of the SMD and SMD-B Models for Ionic Solvation Free Energies

The mean unsigned errors (MUEs) of the aqueous solvation free energies using the two different sets of radii are listed for 52 cations and 60 anions in Table2. Interestingly, the smallest basis set used, 6-31G* yields overall the lowest errors (∼3.4 kcal/mol for M06-2X) in comparison to the other basis sets used (∼4.1–5.0 kcal/mol for M06-2X), which can be attributed to the parametrization of the SMD model based on this basis set.(29) PBE and M06-2X functionals yield lower MUEs for cations using SMD-B (2.4 kcal/mol) and SMD (2.8 kcal/mol) models, respectively. For anions, the M06-2X functional shows MUEs of 4.0 kcal/mol and 5.0 kcal/mol for SMD-B and SMD, respectively, which is the lowest MUE in comparison to the other functionals used. The results in Table2 indicates that SMD-B consistently outperforms the SMD solvation model for predicting the ionic solvation free energies in aqueous media, irrespective of the combination of the basis set and density functional. The results for the 112 ions studied here show that the Bondi radii can decrease the error by ∼0.6 kcal/mol. The average MUE for all ions using the SMD-B and M06-2X/6-31G* method is 3.4 kcal/mol, in contrast with ∼4.0 kcal/mol MUE for the default SMD radii.

Table 2. Mean Unsigned Errors (MUE, in kcal/mol) of Aqueous Ionic Solvation Free Energies Using Bondi and SMD Default Radii (in Brackets) Calculated with Different Basis Sets and Density Functionals

solute	N	PBE	BLYP	B3LYP	M06-2X	PBE0	ωB97XD
6-31G*							
cations	**52**	**2.4 [3.5]**	**2.7 [3.8]**	**2.8 [3.3]**	**2.8 [2.9]**	**2.7 [3.2]**	**2.9 [3.2]**
anions	**60**	**5.6 [6.8]**	**5.9 [7.3]**	**4.8 [5.9]**	**4.0 [5.0]**	**4.5 [5.2]**	**4.3 [5.0]**
all ions	**112**	**4.1 [5.3]**	**4.4 [5.7]**	**3.9 [4.7]**	**3.4 [4.0]**	**3.7 [4.3]**	**3.7 [4.2]**
6-31+G*							
cations	**52**	**3.0 [2.7]**	**3.0 [2.9]**	**3.6 [2.8]**	**3.5 [2.6]**	**3.4 [2.6]**	**3.6 [2.8]**
anions	**60**	**7.3 [8.4]**	**7.7 [8.7]**	**6.0 [7.2]**	**4.6 [5.8]**	**5.1 [6.3]**	**4.6 [5.7]**
all ions	**112**	**5.3 [5.7]**	**5.5 [6.0]**	**4.9 [5.2]**	**4.1 [4.3]**	**4.3 [4.6]**	**4.1 [4.4]**
cc-pVTZ							
cations	**52**	**2.7 [2.7]**	**3.0 [3.5]**	**3.0 [3.2]**	**3.2 [3.1]**	**3.0 [3.1]**	**3.0 [3.2]**
anions	**60**	**6.6 [8.1]**	**7.3 [8.6]**	**5.6 [7.0]**	**6.6 [8.1]**	**5.1 [6.5]**	**4.8 [6.0]**
all ions	**112**	**4.8 [5.6]**	**5.3 [6.2]**	**4.4 [5.2]**	**5.0 [5.8]**	**4.1 [4.9]**	**4.0 [4.7]**
aug-pcseg-2							
cations	**52**	**2.9 [3.3]**	**3.0 [3.5]**	**3.2 [3.4]**	**3.1 [3.3]**	**3.1 [4.4]**	**3.2 [3.4]**
anions	**60**	**8.0 [8.9]**	**9.1 [9.9]**	**7.2 [8.6]**	**5.4 [6.6]**	**6.3 [8.2]**	**5.8 [6.8]**
all ions	**112**	**5.6 [6.3]**	**6.3 [6.9]**	**5.3 [6.2]**	**4.3 [5.1]**	**4.8 [6.4]**	**4.6 [5.2]**
def2-TZVPPD							
cations	**52**	**2.6 [3.3]**	**2.9 [3.4]**	**3.0 [3.2]**	**3.1 [3.1]**	**2.9 [3.1]**	**3.2 [3.2]**
anions	**60**	**8.4 [9.7]**	**9.1 [10.4]**	**7.5 [8.7]**	**5.5 [6.8]**	**6.7 [8.1]**	**5.8 [7.2]**
all ions	**112**	**5.7 [6.7]**	**6.2 [7.2]**	**5.4 [6.1]**	**4.4 [5.1]**	**4.9 [5.8]**	**4.6 [5.3]**

To investigate the performance of the Bondi radii for nonaqueous solvents, the solvation free energies of 220 ionic molecules (Tables S15–S26, SI) with the experimental data (MNSol data set(54)) were calculated using the M06-2X/6-31G* method. The SMD with its default radii outperforms the SMD-B model for all anions in nonaqueous solvents (acetonitrile, dimethyl sulfoxide (DMSO), and methanol, Table3). This phenomenon can be attributed to the more diffused nature of anions, which is in direct contrast with the smaller Bondi radii in comparison to the default intrinsic atomic radii of SMD (Table1).(59)

Table 3. Mean (Un)signed Errors (MUE and MSE, in kcal/mol) of Ionic Solvation Free Energies using Bondi and SMD Default Radii (in Brackets) at M06-2X/6-31G* Level of Theory

solute	*N*	solvent	MUE	MSE
cations	**39**	**MeCN**	**2.7 [7.8]**	**1.4 [7.5]**
anions	**30**	**MeCN**	**18.0 [3.5]**	**−18.0 [−3.1]**
cations	**4**	**DMSO**	**4.0 [8.7]**	**4.0 [8.7]**
anions	**67**	**DMSO**	**16.4 [4.4]**	**−16.4 [−3.0]**
cations	**29**	**MeOH**	**4.3 [2.3]**	**−4.3 [0.0]**
anions	**51**	**MeOH**	**2.7 [2.3]**	**−0.7 [0.6]**
cations	**52**	**H_2O**	**2.8 [2.9]**	**−1.4 [2.4]**
anions	**60**	**H_2O**	**4.0 [5.0]**	**1.8 [4.4]**

Regarding the cations, SMD-B showed better results for acetonitrile and dimethyl sulfoxide (DMSO) solvents. The MUE differences (SMD, SMD-B) for acetonitrile and DMSO are 5.1 and 4.7 kcal/mol in favor of the SMD-B model, respectively. However, in methanol, SMD yields smaller MUE, 2.3 vs 4.3 kcal/mol. The comparison of the mean signed errors (MSE) for organic solvents indicates that the smaller radii of SMD-B lead to systematic underestimation (i.e., more negative than experimental solvation free energies) of the solvation free energies for all anions. However, for anions in water, the calculated values come closer to the experimental data. For cations, water and methanol solvents showed underestimation; at the same time, the values improved for acetonitrile and dimethyl sulfoxide solvents. Among all considered solvents, usage of the Bondi radii is advantageous for aqueous solutions, and, therefore, in the remaining part of this work, we focus on aqueous solvation free energies.

The analysis of the 60 investigated solvation free energies (Table2) suggests that the largest differences between the SMD and SMD-B models are observed for sulfur-containing anions. Table4 contains calculated solvation free energies for six sulfur-containing anions using the M06-2X/6-31G* level of theory. The calculated MUEs for the SMD and SMD-B models are 7.6 and 2.4 kcal/mol, respectively, i.e., using Bondi radii improves the solvation energies of sulfur-containing ions by ∼5.2 kcal/mol compared to the SMD default radii. The only molecule for which SMD showed a better result is hydrogen sulfide clustered with one explicit water molecule.

Table 4. Performance of SMD-B and SMD ($\Delta\Delta G$ = ΔG[calculated] – ΔG[exp.], in kcal/mol) for the Sulfur-Containing Anions Calculated with M06-2X/6-31G*

compound	exp.	$\Delta\Delta G$ [SMD-B]	$\Delta\Delta G$ [SMD]
hydrogen sulfide (cluster)	**−65.5**	**−7.8**	**1.2**
methanethiol	**−73.8**	**−1.8**	**11.8**
ethanethiol	**−71.8**	**−1.9**	**11.6**
1-propanethiol	**−70.5**	**−2.4**	**11.1**
thiophenol	**−63.4**	**−0.6**	**8.4**
dimethyl sulfoxide	**−67.7**	**0.0**	**1.6**
average		**−2.4**	**7.6**

To evaluate the role of the explicit water molecules on this system, the calculations were repeated without a water molecule. Interestingly, the error for SMD-B increased to around −12.8 kcal/mol, whereas the SMD performance improved (0.1 kcal/mol error). The calculations revealed that the S–H bond length decreases by ∼0.4 pm when using the Bondi radii. The change in the bond length, in turn, increases the dipole moment of this molecule from 1.19 to 1.55 D. In contrast to the HS^- anion, the S–C bond length showed ∼1 pm increase for

CH_3SH (methanethiol), EtSH (ethanethiol), ProSH (1-propanethiol), and thiophenol molecules. The differences between hydrogen sulfide and other molecules show that Bondi radii are not reliable for this particular system (HS^-). However, for all molecules, the cavity surface of SMD-B is smaller (Figure 1) and closer to the sulfur atom. This phenomenon can be attributed to the large difference between the Bondi radius of sulfur (1.80 Å) in comparison to the SMD default radius (2.49 Å). It seems that this smaller radius decreases the ability of sulfur to participate in hydrogen bonding. As shown in Figure 1, the calculated hydrogen bond between water and HS^- is ∼13 pm longer with Bondi radii. It should be noted that the average free energy of solvation difference for 21 alcohol and phenol anions is just around 0.3 kcal/mol in favor of the Bondi radii. The radii for oxygen in both SMD-B and SMD are similar (1.52 Å, Table1). Therefore, this difference (∼0.3 kcal/mol) can be attributed to the differences related to the other atoms such as carbon; the radius of carbon in Bondi is ∼0.15 Å smaller than the SMD default radii (Table1).

Figure 1

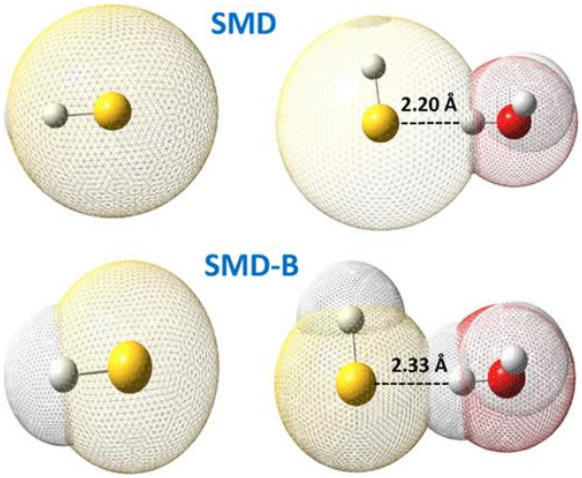

Figure 1. Solvation cavity (M06-2X/6-31G*) for HS^- (left) and HS^-–water cluster (right) anions using SMD and SMD-B models.

Although the focus of this work is on the free energy of solvation of ionic molecules, for completeness, we have also investigated the performance of SMD-B for 22 sulfur-containing neutral molecules using the M06-2X/6-31G* method (Table S2 in the Supporting Information). The results indicated that the SMD-B underestimates the aqueous solvation free energies, with MUE and MSE around 2.8 and −2.8 kcal/mol, respectively, as compared to 1.0 and 0.25 kcal/mol for the SMD solvation model. These results suggest that it may be more advantageous to define two different sets of radii for neutral and ionic molecules.

It is important to note that in addition to including bulk electrostatic effects, implicit solvation models include nonbulk (e.g., hydrogen bonding, dispersion, CH−π, etc.) interactions via the cavitation, dispersion, and solvent structural effects (CDS). The major issue arising here is the significant differences between the magnitude of solvation free energies of neutral and ionic molecules. Indeed, the bulk electrostatic effects have a larger contribution to the solvation free energies of ions than neutral molecules.(29) The difference in nonbulk effects is also significant for ions with opposite charges, which referred to the charge hydration asymmetry.(60,61) Therefore, finding a reasonable balance between the electrostatic and CDS contributions plays an important role in the accurate simulation of solvation effects for both neutral and ionic molecules. As the SMD-B model shows the best performance for the sulfur-containing ionic molecules, we next investigate the effect of Bondi radii on the prediction of thiols pK_a.

Application of the SMD-B Model for Predicting the pK_a Values of Thiols

Schlegel and co-workers tested the accuracy of 175 different DFT functionals for predicting the pK_a values of methanethiol and ethanethiol using the SMD solvation model.(38) They found that the error of the calculated values is almost consistent for all density functionals and that all of the functionals overestimate pK_a values by ∼10 pK_a units. Moreover, they found that scaling of the solvent cavity does not significantly improve the results for thiolates.(38) However, scaling the solvent cavity showed good results for pK_a and oxidation potential values of some nucleobases.(62,63) Finally, they used explicit water molecules to compensate for the deficiencies of the pure implicit-only SMD approach for simulating the short-range hydrogen bonding interactions. Their results indicated that the ωB97XD/6-31+G** level of theory with three water molecules gives the best results among the tested methods. This lower error is achieved at the expense of higher computational cost due to the treatment of explicit water molecules.

The results of Schlegel and co-workers and also the other calculations for predicting the pK_a values of other functional groups(22−28) indicate less satisfactory results of the implicit solvation models for predicting the solvation free energies of ions in the protic solvents.(64) Pomogaeva and Chipman attempted to include the solute–solvent dispersion, Pauli repulsion, and hydrogen bonding effects on the final calculated solvation free energies.(65) Their implicit solvation model, a composite method for implicit representation of the solvent (CMIRS), showed very good results for aqueous solvation free energies of neutral molecules and ions. The MUEs for 60 anions and 52 cations are around 3 and 2 kcal/mol, respectively.

Despite the better performance of CMIRS model in comparison to SMD for ions, the average MUE for six sulfur-containing anions of this model is higher than SMD (8.6 kcal/mol). Recently, You and Herbert reparametrized the original CMIRS parameters to modify the treatment of the dispersion interactions,(66) which decreased the average MUE for six sulfur-containing anions to ∼6.3 kcal/mol (compared to 7.6 kcal/mol of the SMD model, Table4); however, this error is still higher than the average error for other ions (2.9 kcal/mol). These results indicated that the inclusion of additional empirical parameters to the implicit solvation models cannot improve its accuracy for sulfur-containing anions.

To show the direct relationship between the ionic solvation energies of thiols and their pK_a values, we evaluated the applicability of the SMD-B solvation model using a set of 45 thiol molecules(67−73) (Figure S2, SI). The accuracy of the predicted pK_a values can be a good indication of the reliability of the Bondi radii implemented in the SMD solvation model for predicting the acidity of thiols. As evident from Table2, the 6-31G* basis set shows overall the best results for the investigated anions (with MUEs of ∼4.0 and ∼5.0 kcal/mol for M06-2X using Bondi and SMD default radii, respectively). Among the density functionals used, M06-2X, PBE0, and ωB97XD, which showed the lowest MUEs (4.0, 4.5, and 4.3 kcal/mol, respectively), have been selected for the evaluation of the pK_a values of thiols.

The calculated pK_a values are shown in Table S1 in the Supporting Information. M06-2X functional yields the best results for both SMD-B and SMD models, with MUEs of ∼1.08 and ∼7.4 pK_a units. As shown in Figure 2, the Bondi radii decrease the slope of the linear correlation between the calculated and experimental pK_a values from ∼2.0 for SMD to ∼1.25 for SMD-B; in addition, the correlation coefficient R^2 value increased from 0.918 to 0.938. The other two functionals, PBE0 and ωB97XD, show higher MUEs (2.90 and 3.67 pK_a unit, respectively), which agree with the errors from the calculated solvation free energies (Table2) using the same level of theory (see Table S1, SI). Yet, their slopes are close to unity, i.e., 1.26 and 1.17 for PBE0 and ωB97XD functionals, respectively, much smaller than the slopes obtained using SMD default radii, i.e., 2.19 and 2.05 for PBE0 and ωB97XD functionals, respectively. Overall, the Bondi radii showed significantly better performance for predicting the pK_a of thiols in comparison to the SMD default radii. Importantly, these results are independent of the

choice of DFT functional, while improving the predicted values by ~6 pK_a units (see Table S1, Figures S3 and S4 in the Supporting Information).

Figure 2

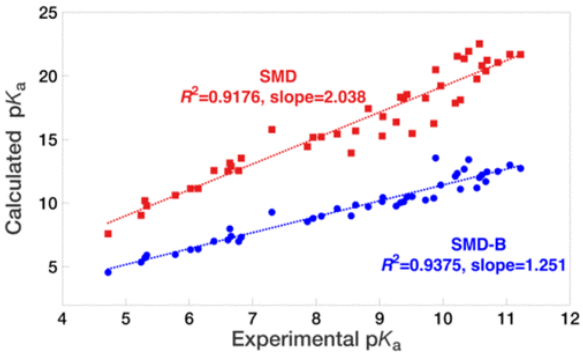

Figure 2. Linear correlation of experimental and calculated pK_a values of 45 thiols employing Bondi radii (SMD-B, blue) and the SMD default radii (SMD, red) at the M06-2X/6-31G* level of theory.

As the M06-2X functional has the highest exact/HF exchange contribution (54%) among the selected functionals, it is conceivable that the inclusion of higher contribution of the HF exchange improves the calculated solvation free energies/pK_a values. To verify this hypothesis, we calculated pK_a values with M06-HF/6-31G* that includes 100% HF exchange. Indeed, we found that compared to M06-2X, the M06-HF functional yields lower MUEs for the set of 45 selected thiols studied (~0.84 pK_a unit). However, the slope of the linear correlation between calculated and experimental pK_as increased to ~1.28 (Table S33 and Figure S5 in the Supporting Information). Also, the R^2 value decreased from 0.9375 for M06-2X to 0.8785 for M06-HF. The decrease in the HF exchange contribution to 26% (M06 functional) and 0% (M06-L functional) increases the MUE to 2.53 and 2.91 pK_a unit, respectively (Tables S34 and S35, Figures S6 and S7, SI). Therefore, it appears that the M06-2X has the optimal amount of HF exchange correlation among the examined functionals.

Conclusions

In this study, we investigated the utility of Bondi radii with the SMD implicit solvation model for a set of 112 ions (60 anions and 52 cations). We found that using Bondi radii instead of the default SMD radii leads to more accurate values of the calculated aqueous solvation free energies of ions, anions in particular, where the MUE decreases by ~1 kcal/mol. This effect is the most pronounced for the sulfur-containing molecules (~5 kcal/mol). Motivated by the better performance of the SMD-B approach, we studied its application for predicting the pK_a values of thiols. A set of 45 thiols with pK_a values in the range of 4–12 have been selected, and their pK_a values were calculated. The usage of the Bondi radii decreases the error of calculated pK_a values from 7 to 1 pK_a unit. Thus, the acceptable error is achieved without using any thermodynamic cycle or explicit water molecules. Finally, we conclude that the improved implicit solvation models should employ radii that are specifically parameterized for a given charge state of a solute and the type of a solvent.

Supporting Information

The Supporting Information is available free of charge on the ACS Publications website at DOI: 10.1021/acs.jpca.9b02340.

Calculated solvation free energies for all ions and neutral molecules and pK_a of thiols; structures of 45 thiols; generic input file for running Gaussian with Bondi radii and optimized geometries of all thiols (PDF)

pdf

jp9b02340_si_001.pdf (1.1 MB)

Author Contributions

The manuscript was written through the contributions of all authors.

The authors declare no competing financial interest.

Note Added in Proof

In a recent paper (Ref. (18)), Lian et al. also report superior performance of SMD with Bondi radii for thiols, further improved by radii scaling.

Terms & Conditions

Acknowledgments

This work used the high-performance computing cluster at the Extreme Science and Engineering Discovery Environment (XSEDE) supported by NSF grant ACI-1053575. Q.K.T. is a recipient of the National Science Foundation (NSF) CAREER award CHE-1255641 and Marquette University Way-Klinger Sabbatical Award. The authors would like to thank anonymous reviewers for useful suggestions.

References

1 Ho, J.; Coote, M. L. First-Principles Prediction of Acidities in the Gas and Solution Phase. *Wiley Interdiscip. Rev.: Comput. Mol. Sci.* **2011**, *1*, 649– 660, DOI: 10.1002/wcms.43

2 Seybold, P. G.; Shields, G. C. Computational Estimation of PK a Values. *Wiley Interdiscip. Rev.: Comput. Mol. Sci.* **2015**, *5*, 290– 297, DOI: 10.1002/wcms.1218

3 Ho, J.; Coote, M. L. A Universal Approach for Continuum Solvent pK_a Calculations: Are We There Yet?. *Theor. Chem. Acc.* **2010**, *125*, 3– 21, DOI: 10.1007/s00214-009-0667-0

4 Shields, G. C.; Seybold, P. G. *Computational Approaches for the Prediction of pK_a Values*; CRC Press: Boca Raton, FL, **2013**.

5 Cancès, E.; Mennucci, B.; Tomasi, J. A New Integral Equation Formalism for the Polarizable Continuum Model: Theoretical Background and Applications to Isotropic and Anisotropic Dielectrics. *J. Chem. Phys.* **1997**, *107*, 3032– 3041, DOI: 10.1063/1.474659

6 Cossi, M.; Rega, N.; Scalmani, G.; Barone, V. Energies, Structures, and Electronic Properties of Molecules in Solution with the C-PCM Solvation Model. *J. Comput. Chem.* **2003**, *24*, 669– 681, DOI: 10.1002/jcc.10189

7 Klamt, A.; Schüürmann, G. COSMO: A New Approach to Dielectric Screening in Solvents with Explicit Expressions for the Screening Energy and Its Gradient. *J. Chem. Soc., Perkin Trans. 2* **1993**, *5*, 799– 805, DOI: 10.1039/P29930000799

8 Miertuš, S.; Scrocco, E.; Tomasi, J. Electrostatic Interaction of a Solute with a Continuum. A Direct Utilizaion of AB Initio Molecular Potentials for the Prevision of Solvent Effects. *Chem. Phys.* **1981**, *55*, 117– 129, DOI: 10.1016/0301-0104(81)85090-2

9 Miertuš, S.; Tomasi, J. Approximate Evaluations of the Electrostatic Free Energy and Internal Energy Changes in Solution Processes. *Chem. Phys.* **1982**, *65*, 239– 245, DOI: 10.1016/0301-0104(82)85072-6

10 Marenich, A. V.; Olson, R. M.; Kelly, C. P.; Cramer, C. J.; Truhlar, D. G. Self-Consistent Reaction Field Model for Aqueous and Nonaqueous Solutions Based on Accurate Polarized Partial Charges. *J. Chem. Theory Comput.* **2007**, *3*, 2011– 2033, DOI: 10.1021/ct7001418

11 Marenich, A. V.; Cramer, C. J.; Truhlar, D. G. Generalized Born Solvation Model SM12. *J. Chem. Theory Comput.* **2013**, *9*, 609– 620, DOI: 10.1021/ct300900e

12 Tucker, S. C.; Truhlar, D. G. Generalized Born Fragment Charge Model for Solvation Effects as a Function of Reaction Coordinate. *Chem. Phys. Lett.* **1989**, *157*, 164– 170, DOI: 10.1016/0009-2614(89)87227-6

13 Cramer, C. J.; Truhlar, D. G. General Parameterized SCF Model for Free Energies of Solvation in Aqueous Solution. *J. Am. Chem. Soc.* **1991**, *113*, 8305– 8311, DOI: 10.1021/ja00022a017

14 Mu, W.-H.; Chasse, G. A.; Fang, D.-C. Test and Modification of the van Der Waals' Radii Employed in the Default PCM Model. *Int. J. Quantum Chem.* **2008**, *108*, 1422– 1434, DOI: 10.1002/qua.21674

15 Tao, J.-Y.; Mu, W.-H.; Chass, G. A.; Tang, T.-H.; Fang, D.-C. Balancing the Atomic Waistline: Isodensity-Based Scrf Radii for Main-Group Elements and Transition Metals. *Int. J. Quantum Chem.* **2013**, *113*, 975– 984, DOI: 10.1002/qua.24065

16 Kříž, K.; Řezáč, J. Reparametrization of the COSMO Solvent Model for Semiempirical Methods PM6 and PM7. *J. Chem. Inf. Model.* **2019**, *59*, 229– 235, DOI: 10.1021/acs.jcim.8b00681

17 Engelage, E.; Schulz, N.; Heinen, F.; Huber, S. M.; Truhlar, D. G.; Cramer, C. J. Refined SMD Parameters for Bromine and Iodine Accurately Model Halogen-Bonding Interactions in Solution. *Chem. - Eur. J.* **2018**, *24*, 15983– 15987, DOI: 10.1002/chem.201803652

18 Lian, P.; Johnston, R. C.; Parks, J. M.; Smith, J. C. Quantum Chemical Calculation of pK_as of Environmentally Relevant Functional Groups: Carboxylic Acids, Amines, and Thiols in Aqueous Solution. *J. Phys. Chem. A* **2018**, *122*, 4366– 4374, DOI: 10.1021/acs.jpca.8b01751

19 Sviatenko, L. K.; Gorb, L.; Hill, F. C.; Leszczynska, D.; Leszczynski, J. Theoretical Study of One-Electron Reduction And Oxidation Potentials of N-Heterocyclic Compounds. *Chem. Heterocycl. Compd.* **2014**, *50*, 311– 318, DOI: 10.1007/s10593-014-1484-5

20 Bondi, A. Van Der Waals Volumes and Radi. *J. Phys. Chem. A* **1964**, *68*, 441– 451, DOI: 10.1021/j100785a001

21 Ho, J. Are Thermodynamic Cycles Necessary for Continuum Solvent Calculation of pK_as and Reduction Potentials?. *Phys. Chem. Chem. Phys.* **2015**, *17*, 2859– 2868, DOI: 10.1039/C4CP04538F

22 Pliego, J. R.; Riveros, J. M. Theoretical Calculation of pK_a Using the Cluster–Continuum Model. *J. Phys. Chem. A* **2002**, *106*, 7434– 7439, DOI: 10.1021/jp025928n

23 Adam, K. R. New Density Functional and Atoms in Molecules Method of Computing Relative pK_a Values in Solution. *J. Phys. Chem. A* **2002**, *106*, 11963– 11972, DOI: 10.1021/jp026577f

24 Kelly, C. P.; Cramer, C. J.; Truhlar, D. G. Adding Explicit Solvent Molecules to Continuum Solvent Calculations for the Calculation of Aqueous Acid Dissociation Constants. *J. Phys. Chem. A* **2006**, *106*, 2493– 2499, DOI: 10.1021/jp055336f

25 Bryantsev, V. S.; Diallo, M. S.; Goddard, W. A., III Calculation of Solvation Free Energies of Charged Solutes Using Mixed Cluster/Continuum Models. *J. Phys. Chem. B* **2008**, *112*, 9709– 9719, DOI: 10.1021/jp802665d

26 da Silva, E. F.; Svendsen, H. F.; Merz, K. M. Explicitly Representing the Solvation Shell in Continuum Solvent Calculations. *J. Phys. Chem. A* **2009**, *113*, 6404– 6409, DOI: 10.1021/jp809712y

27 Zhang, S. A Reliable and Efficient First Principles-Based Method for Predicting pK_a Values. III. Adding Explicit Water Molecules: Can the Theoretical Slope Be Reproduced and pK_a Values Predicted More Accurately?. *J. Comput. Chem.* **2012**, *33*, 517– 526, DOI: 10.1002/jcc.22886

28 Gupta, M.; da Silva, E. F.; Svendsen, H. F. Explicit Solvation Shell Model and Continuum Solvation Models for Solvation Energy and pK_a Determination of Amino Acids. *J. Chem. Theory Comput.* **2013**, *9*, 5021– 5037, DOI: 10.1021/ct400459y

29 Marenich, A. V.; Cramer, C. J.; Truhlar, D. G. Universal Solvation Model Based on Solute Electron Density and on a Continuum Model of the Solvent Defined by the Bulk Dielectric Constant and Atomic Surface Tensions. *J. Phys. Chem. B* **2009**, *113*, 6378– 6396, DOI: 10.1021/jp810292n

30 Ho, J.; Ertem, M. Z. Calculating Free Energy Changes in Continuum Solvation Models. *J. Phys. Chem. B* **2016**, *120*, 1319– 1329, DOI: 10.1021/acs.jpcb.6b00164

31 Miguel, E. L. M.; Silva, P. L.; Pliego, J. R. Theoretical Prediction of pK_a in Methanol: Testing SM8 and SMD Models for Carboxylic Acids, Phenols, and Amines. *J. Phys. Chem. B* **2014**, *118*, 5730– 5739, DOI: 10.1021/jp501379p

32 Matsui, T.; Shigeta, Y.; Morihashi, K. Assessment of Methodology and Chemical Group Dependences in the Calculation of the pK_a for Several Chemical Groups. *J. Chem. Theory Comput.* **2017**, *13*, 4791– 4803, DOI: 10.1021/acs.jctc.7b00587

33 Nazemi, A.; Cundari, T. R. Control of C–H Bond Activation by Mo-Oxo Complexes: pK_a or Bond Dissociation Free Energy (BDFE)?. *Inorg. Chem.* **2017**, *56*, 12319– 12327, DOI: 10.1021/acs.inorgchem.7b01738

34 Yu, H.-Z.; Yang, Y.-M.; Zhang, L.; Dang, Z.-M.; Hu, G.-H. Quantum-Chemical Predictions of pK_a's of Thiols in DMSO. *J. Phys. Chem. A* **2014**, *118*, 606– 622, DOI: 10.1021/jp410274n

35 Sutton, C. C. R.; Franks, G. V.; da Silva, G. First Principles pK_a Calculations on Carboxylic Acids Using the SMD Solvation Model: Effect of Thermodynamic Cycle, Model Chemistry, and Explicit Solvent Molecules. *J. Phys. Chem. B* **2012**, *116*, 11999– 12006, DOI: 10.1021/jp305876r

36 Haworth, N. L.; Wang, Q.; Coote, M. L. Modeling Flexible Molecules in Solution: A pK_a Case Study. *J. Phys. Chem. A* **2017**, *121*, 5217– 5225, DOI: 10.1021/acs.jpca.7b04133

37 Charmet, A. P.; Quartarone, G.; Ronchin, L.; Tortato, C.; Vavasori, A. Quantum Chemical Investigation on Indole: Vibrational Force Field and Theoretical Determination of Its Aqueous pK_a Value. *J. Phys. Chem. A* **2013**, *117*, 6846– 6858, DOI: 10.1021/jp4049692

38 Thapa, B.; Schlegel, H. B. Density Functional Theory Calculation of pK_a's of Thiols in Aqueous Solution Using Explicit Water Molecules and the Polarizable Continuum Model. *J. Phys. Chem. A* **2016**, *120*, 5726– 5735, DOI: 10.1021/acs.jpca.6b05040

39 Thapa, B.; Schlegel, H. B. Calculations of pK_a's and Redox Potentials of Nucleobases with Explicit Waters and Polarizable Continuum Solvation. *J. Phys. Chem. A* **2015**, *119*, 5134– 5144, DOI: 10.1021/jp5088866

40 Thapa, B.; Schlegel, H. B. Theoretical Calculation of pK_a's of Selenols in Aqueous Solution Using an Implicit Solvation Model and Explicit Water Molecules. *J. Phys. Chem. A* **2016**, *120*, 8916– 8922, DOI: 10.1021/acs.jpca.6b09520

41 Thapa, B.; Schlegel, H. B. Improved pK_a Prediction of Substituted Alcohols, Phenols, and Hydroperoxides in Aqueous Medium Using Density Functional Theory and a Cluster-Continuum Solvation Model. *J. Phys. Chem. A* **2017**, *121*, 4698– 4706, DOI: 10.1021/acs.jpca.7b03907

42 Frisch, M. J.; Trucks, G. W.; Schlegel, H. B.; Scuseria, G. E.; Robb, M. A.; Cheeseman, J. R.; Scalmani, G.; Barone, V.; Mennucci, B.; Petersson, G. A.; Nakatsuji, H.; Caricato, M.; Li, X.; Hratchian, H. P.; Izmaylov, A. F.; Bloino, J.; Zheng, G.; Sonnenberg, J. L.; Hada, M.; Ehara, M.; Toyota, K.; Fukuda, R.; Hasegawa, J.; Ishida, M.; Nakajima, T.; Honda, Y.; Kitao, O.; Nakai, H.; Vreven, T.; Montgomery, J. A., Jr.; Peralta, J. E.; Ogliaro, F.; Bearpark, M.; Heyd, J. J.; Brothers, E.; Kudin, K. N.; Staroverov, V. N.; Kobayashi, R.; Normand, J.; Raghavachari, K.; Rendell, A.; Burant, J. C.; Iyengar, S. S.; Tomasi, J.; Cossi, M.; Rega, N.; Millam, J. M.; Klene, M.; Knox, J. E.; Cross, J. B.; Bakken, V.; Adamo, C.; Jaramillo, J.; Gomperts, R.; Stratmann, R. E.; Yazyev, O.; Austin, A. J.; Cammi, R.; Pomelli, C.; Ochterski, J. W.; Martin, R. L.; Morokuma, K.; Zakrzewski, V. G.; Voth, G. A.; Salvador, P.; Dannenberg, J. J.; Dapprich, S.; Daniels, A. D.; Farkas, Ö.; Foresman, J. B.; Ortiz, J. V.; Cioslowski, J.; Fox, D. J. *Gaussian 09*; Gaussian, Inc.: Wallingford CT, **2009**.

43 Ben-Naim, A. *Solvation Thermodynamics*; Springer: Boston, MA, **1987**.

44 Perdew, J. P.; Burke, K.; Ernzerhof, M. Generalized Gradient Approximation Made Simple. *Phys. Rev. Lett.* **1996**, *77*, 3865– 3868, DOI: 10.1103/PhysRevLett.77.3865

45 Becke, A. D. Density-Functional Exchange-Energy Approximation with Correct Asymptotic Behavior. *Phys. Rev. A* **1988**, *38*, 3098– 3100, DOI: 10.1103/PhysRevA.38.3098

46 Adamo, C.; Barone, V. Toward Reliable Density Functional Methods without Adjustable Parameters: The PBE0 Model. *J. Chem. Phys.* **1999**, *110*, 6158– 6170, DOI: 10.1063/1.478522

47 Chai, J.-D.; Head-Gordon, M. Long-Range Corrected Hybrid Density Functionals with Damped Atom–Atom Dispersion Corrections. *Phys. Chem. Chem. Phys.* **2008**, *10*, 6615– 6620, DOI: 10.1039/b810189b

48 Zhao, Y.; Truhlar, D. G. The M06 Suite of Density Functionals for Main Group Thermochemistry, Thermochemical Kinetics, Noncovalent Interactions, Excited States, and Transition Elements: Two New Functionals and Systematic Testing of Four M06-Class Functionals and 12 Other Function. *Theor. Chem. Acc.* **2008**, *120*, 215– 241, DOI: 10.1007/s00214-007-0310-x

49 Dunning, T. H. Gaussian Basis Sets for Use in Correlated Molecular Calculations. I. The Atoms Boron through Neon and Hydrogen. *J. Chem. Phys.* **1989**, *90*, 1007– 1023, DOI: 10.1063/1.456153

50 Jensen, F. Unifying General and Segmented Contracted Basis Sets. Segmented Polarization Consistent Basis Sets. *J. Chem. Theory Comput.* **2014**, *10*, 1074– 1085, DOI: 10.1021/ct401026a

51 Weigend, F. Accurate Coulomb-Fitting Basis Sets for H to Rn. *Phys. Chem. Chem. Phys.* **2006**, *8*, 1057– 1065, DOI: 10.1039/b515623h

52 Zhao, Y.; Truhlar, D. G. Density Functional for Spectroscopy: No Long-Range Self-Interaction Error, Good Performance for Rydberg and Charge-Transfer States, and Better Performance on Average than B3LYP for Ground States. *J. Phys. Chem. A* **2006**, *110*, 13126– 13130, DOI: 10.1021/jp066479k

53 Zhao, Y.; Truhlar, D. G. A New Local Density Functional for Main-Group Thermochemistry, Transition Metal Bonding, Thermochemical Kinetics, and Noncovalent Interactions. *J. Chem. Phys.* **2006**, *125*, 194101 DOI: 10.1063/1.2370993

54 Marenich, A. V.; Kelly, C. P.; Thompson, J. D.; Hawkins, G. D.; Chambers, C. C.; Giesen, D. J.; Winget, P.; Cramer, C. J.; Truhlar, D. G. *Minnesota Solvation Database*, version 2012; University of Minnesota: Minneapolis, **2012**.

55 Palascak, M. W.; Shields, G. C. Accurate Experimental Values for the Free Energies of Hydration of H^+, OH^-, and H_3O^+. *J. Phys. Chem. A* **2004**, *108*, 3692– 3694, DOI: 10.1021/jp049914o

56 Kelly, C. P.; Cramer, C. J.; Truhlar, D. G. Aqueous Solvation Free Energies of Ions and Ion–Water Clusters Based on an Accurate Value for the Absolute Aqueous Solvation Free Energy of the Proton. *J. Phys. Chem. B* **2006**, *110*, 16066– 16081, DOI: 10.1021/jp063552y

57 Isse, A. A.; Gennaro, A. Absolute Potential of the Standard Hydrogen Electrode and the Problem of Interconversion of Potentials in Different Solvents. *J. Phys. Chem. B* **2010**, *114*, 7894– 7899, DOI: 10.1021/jp100402x

58 Marenich, A. V.; Ho, J.; Coote, M. L.; Cramer, C. J.; Truhlar, D. G. Computational Electrochemistry: Prediction of Liquid-Phase Reduction Potentials. *Phys. Chem. Chem. Phys.* **2014**, *16*, 15068– 15106, DOI: 10.1039/C4CP01572J

59 Cramer, C. J. *Essentials of Computational Chemistry: Theories and Models*, 2nd ed.; Wiley, **2004**.

60 Mukhopadhyay, A.; Fenley, A. T.; Tolokh, I. S.; Onufriev, A. V. Charge Hydration Asymmetry: The Basic Principle and How to Use It to Test and Improve Water Models. *J. Phys. Chem. B* **2012**, *116*, 9776– 9783, DOI: 10.1021/jp305226j

61 Mukhopadhyay, A.; Aguilar, B. H.; Tolokh, I. S.; Onufriev, A. V. Introducing Charge Hydration Asymmetry into the Generalized Born Model. *J. Chem. Theory Comput.* **2014**, *10*, 1788– 1794, DOI: 10.1021/ct4010917

62 Verdolino, V.; Cammi, R.; Munk, B. H.; Schlegel, H. B. Calculation of pK_a Values of Nucleobases and the Guanine Oxidation Products Guanidinohydantoin and Spiroiminodihydantoin Using Density Functional Theory and a Polarizable Continuum Model. *J. Phys. Chem. B* **2008**, *112*, 16860– 16873, DOI: 10.1021/jp8068877

63 Psciuk, B. T.; Lord, R. L.; Munk, B. H.; Schlegel, H. B. Theoretical Determination of One-Electron Oxidation Potentials for Nucleic Acid Bases. *J. Chem. Theory Comput.* **2012**, *8*, 5107– 5123, DOI: 10.1021/ct300550x

64 Pliego, J. R.; Riveros, J. M. The Cluster–Continuum Model for the Calculation of the Solvation Free Energy of Ionic Species. *J. Phys. Chem. A* **2001**, *105*, 7241– 7247, DOI: 10.1021/jp004192w

65 Pomogaeva, A.; Chipman, D. M. Hydration Energy from a Composite Method for Implicit Representation of Solvent. *J. Chem. Theory Comput.* **2014**, *10*, 211– 219, DOI: 10.1021/ct400894j

66 You, Z.-Q.; Herbert, J. M. Reparameterization of an Accurate, Few-Parameter Implicit Solvation Model for Quantum Chemistry: Composite Method for Implicit Representation of Solvent, CMIRS v. 1.1. *J. Chem. Theory Comput.* **2016**, *12*, 4338– 4346, DOI: 10.1021/acs.jctc.6b00644

67 Hupe, D. J.; Jencks, W. P. Nonlinear Structure-Reactivity Correlations. Acyl Transfer between Sulfur and Oxygen Nucleophiles. *J. Am. Chem. Soc.* **1977**, *99*, 451– 464, DOI: 10.1021/ja00444a023

68 Arnold, A. P.; Canty, J. Methylmercury(II) Sulfhydryl Interactions. Potentiometric Determination of the Formation Constants for Complexation of Methylmercury(II) by Sulfhydryl Containing Amino Acids and Related Molecules, Including Glutathione. *Can. J. Chem.* **1983**, *61*, 1428– 1434, DOI: 10.1139/v83-250

69 Kreevoy, M. M.; Harper, E. T.; Duvall, R. E.; Wilgus, H. S.; Ditsch, L. T. Inductive Effects on the Acid Dissociation Constants of Mercaptans 1. *J. Am. Chem. Soc.* **2005**, *82*, 4899– 4902, DOI: 10.1021/ja01503a037

70 Kreevoy, M. M.; Eichinger, B. E.; Stary, F. E.; Katz, E. A.; Sellstedt, J. H. The Effect of Structure on Mercaptan Dissociation Constants. *J. Org. Chem.* **1964**, *29*, 1641– 1642, DOI: 10.1021/jo01029a515

71 Irving, R. J.; Nelander, L.; Wadsö, I.Thermodynamics of the Ionization of Some Thiols in Aqueous Solution. *Acta Chem. Scand.* **1964**, *18*, 769– 787, DOI: 10.3891/acta.chem.scand.18-0769

72 De Maria, P.; Fini, A.; Hall, F. M. Thermodynamic Acid Dissociation Constants of Aromatic Thiols. *J. Chem. Soc., Perkin Trans. 2* **1973**, *0*, 1971– 1973, DOI: 10.1039/p29730001969

73 Tsonopoulos, C.; Coulson, D. M.; Lawrence, B. I. Ionization Constants of Water Pollutants. *J. Chem. Eng. Data* **1976**, *21*, 190– 193, DOI: 10.1021/je60069a008